arXiv:0901.2026v2 [astro-ph.SR] 3 Feb 2009

TRIGGERING ERUPTIVE MASS EJECTION IN LUMINOUS BLUE VARIABLES

Amos Harpaz and Noam Soker[1]

ABSTRACT

We study the runaway mass loss process of major eruptions of luminous blue variables (LBVs) stars, such as the 1837-1856 Great Eruption of η Carinae. We follow the evolution of a massive star with a spherical stellar evolution numerical code. After the star exhausted most of the hydrogen in the core and had developed a large envelope, we remove mass at a rate of $1 M_{\odot}$ yr^{-1} from the outer envelope for 20 years. We find that after removing a small amount of mass at a high rate, the star contracts and releases a huge amount of gravitational energy. We suggest that this energy can sustain the high mass loss rate. The triggering of this runaway mass loss process might be a close stellar companion or internal structural changes. We show that a strong magnetic field region can be built in the radiative zone above the convective core of the evolved massive star. When this magnetic energy is released it might trigger a fast removal of mass, and by that trigger an eruption. Namely, LBV major eruptions might be triggered by magnetic activity cycles. The prediction is that LBV stars that experience major eruptions should be found to have a close companion and/or have signatures of strong magnetic activity during or after the eruption.

1. INTRODUCTION

Luminous Blue Variables (LBVs) are massive hot luminous stars. They posses very strong winds that exhibit irregular variabilities on time scales ranging from days to years. On top of these variations, LBVs experience extreme mass loss rate episodes (e.g., Smith & Owocki 2006; Owocki & van Marle 2009, and references therein), e.g., the 19th century eruptions of η Carinae (Humphreys et al. 1999), where a mass of $\sim 10 - 20 M_{\odot}$ was lost (Smith et al. 2003b; Smith 2006; Smith & Owocki 2006; Smith & Ferland 2007). These eruptions cannot be accounted for by the regular stellar luminosity, and they require some

[1]Department of Physics, Technion−Israel Institute of Technology, Haifa 32000 Israel; phr89ah@physics.technion.ac.il; soker@physics.technion.ac.il.

extra energy source, e.g., internal structural change in the star, that might even increase the stellar luminosity above the Eddington limit (Owocki & van Marle 2009). However, part, or even all, of the increase in the luminosity of η Car in the 1837-1856 Great Eruption could have come from gravitational energy of the mass accreted by the secondary star (Soker 2007). The accretion of mass onto the secondary star can explain also the kinetic energy of the Homunculus (Soker 2007); the Homunculus is the bipolar nebula of η Car that was formed in the Great Eruption (Davidson & Humphreys 1997).

The influence of radiation on the mass loss process of stars near their Eddington luminosity limit in relation to LBV eruptions is discussed by van Marle et al. (2008, 2009) and Owocki & van Marle (2009). In particular, they discuss how the extended porosity formalism (Shaviv 1998, 2000) can account for the Great Eruption of η Car (Owocki et al. 2004; van Marle et al. 2008, 2009). In the present paper we do not deal with the interaction of radiation with matter. We rather limit ourself to discuss the possible instability process that can lead to the release of a huge amount of energy by internal structural change.

One of the significant differences between our approach and most other studies of the Great Eruption of η Car concerns the energy of the Homunculus. While most studies (e.g., Smith 2006) attribute the entire energy source to the primary enhanced luminosity, we take the view that most of the kinetic energy of the Homunculus results from two opposite jets that were blown by the companion during the Great Eruption. The companion blew the jets as it accreted mass from the primary dense wind via an accretion disk (Soker 2007). Therefore, we do not deal with the energy of the homunculus, but only with the energy that is required to unbind a mass of $\sim 10-20 M_{\odot}$ during the Great Eruption of η Car, and similar LBV eruptions. The same jets can account for fast ejecta that were blown from the η Car binary system (Smith & Morse 2004).

The mass of $\sim 10-20 M_{\odot}$ (Smith et al. 2003b; Smith & Ferland 2007) that was ejected in the Great Eruption resides in the outer part of the radiative outer region of LBV stars. In section 2 we build a stellar model that has a similar structure to that of η Car before the Great Eruption, and discuss some of its properties. Soker (2007) already speculated that the Great Eruption of η Car was triggered by disturbances in the outer boundary of the inner convective region, most likely by magnetic activity, that expelled the outer radiative zone. Soker (2007) further mentioned that one way to form an extended envelope is by the contraction of the inner layers. In section 3 we go one step further and show that indeed, the removal of the outer region of the star causes the star to shrink and release a huge amount of gravitational energy. Earlier suggestions for the cause of LBV instability was summarized by Humphreys & Davidson (1994). Some of them, e.g., the geyser model of Maeder (1992), cannot work for a hot star like η Car. As we show, our model works for blue stars. In section

4 we discuss in more detail the possibility that the initial mass removal in LBV outbursts is triggered by magnetic activity. We summarize in section 5.

2. STELLAR STRUCTURE

We evolve a spherical stellar model with the same evolutionary code that was used by us in previous studies over the years (for detail see Soker & Harpaz 1999). We start at $t = 0$ with a zero-age main sequence star of mass $M_0 = 190 M_\odot$. Mass loss is not a major part of our study as we are interested in the stellar model toward the end of the main sequence. We simply set the mass loss rate to be $\dot{M} = 2 \times 10^{-5} M_\odot$ yr^{-1} (for more detail on the evolutionary track of massive stars the reader can consult, e.g., Meynet & Maeder 2003, 2005). The mass, luminosity, and effective temperature, at 4 evolutionary points are $[M(M_\odot), L(10^6 L_\odot), T_e(10^4 K)] = (190, 3, 5.7)$, $(160, 3, 5.1)$, $(150, 3, 4.4)$, and $(139, 3, 1.6)$. The luminosity does not evolve much, but as the hydrogen in the core is close to exhaustion the envelope swells and the effective temperature decreases (see also Smith & Conti 2008). In Fig. 1 we show the stellar structure at $t = 0$ and at $t = 2.55$ Myr.

Most relevant to us is the entropy profile. The regions where the entropy profile is flat (actually decreasing very slowly) are convective regions. At early times the star is almost completely convective. At later times the entropy is flat in the inner $\sim 80 M_\odot$. The outer regions are mainly radiative. Above the inner convective region the entropy increases substantially with mass (and radius). Then, in the outer $\sim 15 - 20 M_\odot$ the profile becomes shallow, and a second convective region exists there. At late times most of the volume of the envelope is an outer extended region with very low density ($\sim 10^{-7} - 10^{-6}$ g cm^{-3}) that contains a relatively small amount of mass ($< 1 M_\odot$).

The evolutionary numerical code calculates the entropy S_e using the full equation of state. To further elaborate on the entropy behavior to be used later, we examine the quantity $S_\gamma = P \rho^{\gamma_{\rm ad}}$. As evident from Fig. 2, in the massive radiative region above the convective core a value of $\gamma_{\rm ad} = 1.33$ accurately describes the rapid entropy rise. In Fig. 2 we plot the logarithm of the pressure and of the density, the mass, the accurate entropy calculate by the stellar code S_e, and of S_γ for $\gamma_{\rm ad} = 4/3$ (units are given in the caption), as function of stellar radius for the second model shown in Fig. 1. We note again the rapid rise in the entropy from the core, and then the flattening in the outer $\sim 15 - 20 M_\odot$, where a second convective region resides in the region $22 \lesssim r \lesssim 28 R_\odot$. The very extended outer region is not shown, as it contains a small amount of mass $< 1 M_\odot$.

The important property to take from the graphs is that the mass expelled in eruptions

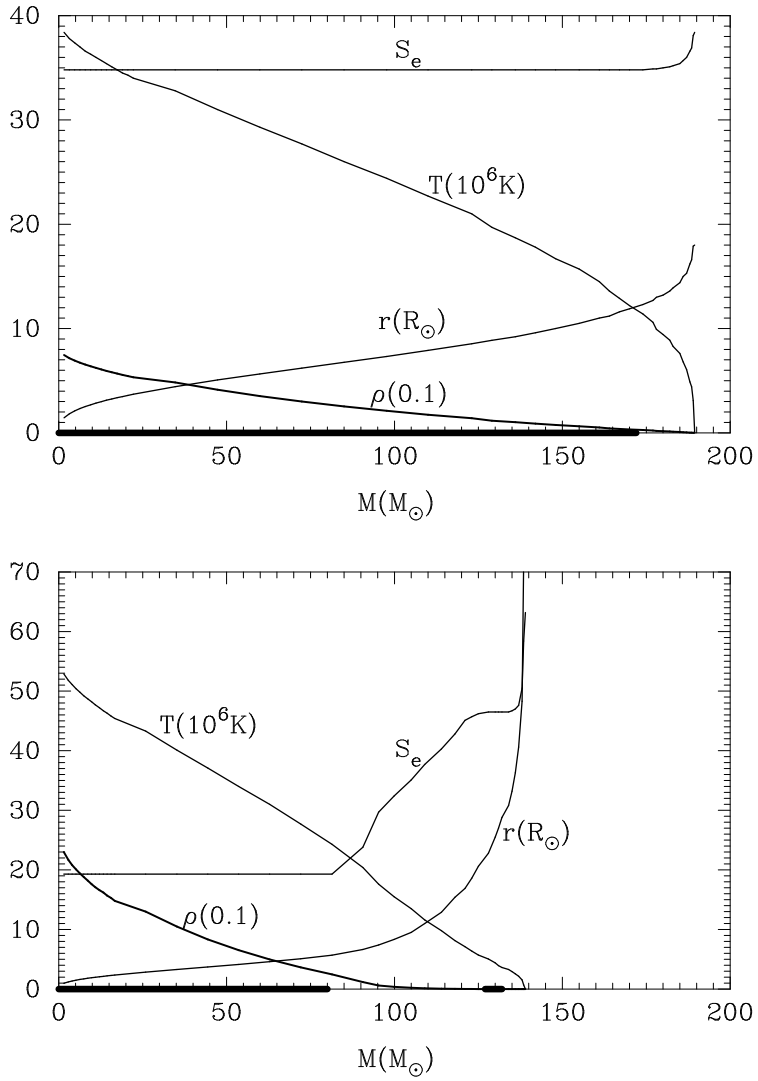

Fig. 1.— Density (in units of 0.1 g cm^{-3}), temperature (in units of 10^6 K), entropy S_e (in relative units), and radius (in solar radii), as function of mass for two evolutionary times: $t = 0$ on the upper panel and $t = 2.55 \times 10^6$ yr in the lower panel. The two models have $[M(M_\odot), L(10^6 L_\odot), T_e(10^4 K)] = (190, 3, 5.7)$, and $(139, 3, 1.6)$, respectively. The thick lines on the horizontal axis mark the convective regions. In the lower panel the photospheric radius is $220 R_\odot$, and it is outside the graph.

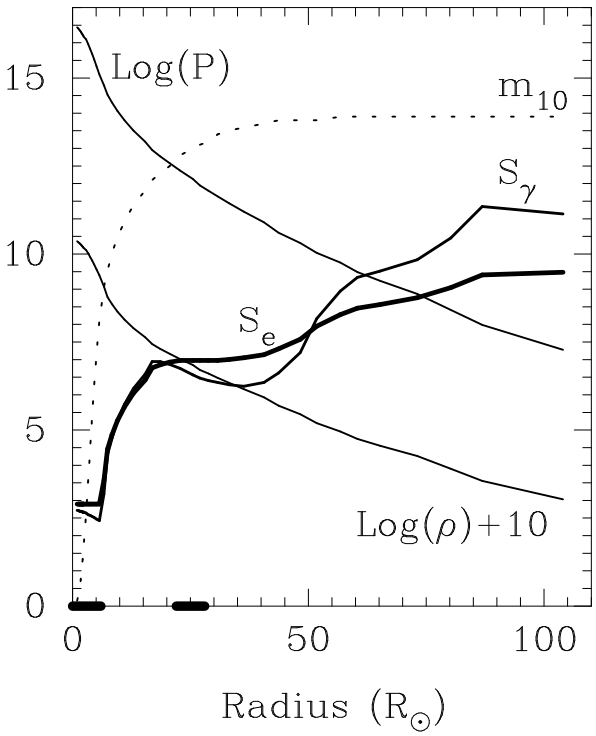

Fig. 2.— Logarithm of the density, $\log\rho(g\ \mathrm{cm}^{-3}) + 10$, of the pressure, in c.g.s units, mass in units of $10M_\odot$, scaled accurate entropy from the stellar numerical code S_e, and $S_\gamma \equiv 3.0\times10^{-16}P\rho^{-4/3}$ in c.g.s. units, as function of radius in solar radii. There are two convective regions marked by thick lines on the horizontal axis. One is in the core $r \lesssim 6R_\odot$ ($M \lesssim 80M_\odot$), and the other at $22 \lesssim r \lesssim 28R_\odot$ ($127 \lesssim M \lesssim 132M_\odot$). the photosphere is at a radius of $R_{\rm ph} = 220R_\odot$, but the region above $r = 105R_\odot$ contains very little mass, and is not shown in this figure. The model is the one drawn in the lower panel of Fig. 1: $[M(M_\odot), L(10^6L_\odot), T_e(10^4K)] = (139, 3, 1.6)$.

of LBVs, such as the Great Eruption of η Car, is a high-entropy gas.

3. THE ERUPTION PHASE

Stars with a radiative envelope shrink as they loss mass on a time scale shorter than the thermal time scale (Webbink 1976; Heisler & Alcock 1986; Maeder 1992). The release of gravitational energy by the contracting envelope can lead to an increase in the mass loss rate, resulting in a runaway mass loss process.

To examine the behavior of our model we start with the star at the evolutionary point $[M(M_\odot), L(10^6 L_\odot), T_e(10^4 K)] = (139, 3, 1.6)$, and we remove $\Delta M_{\rm burst} = 20 M_\odot$ with a constant mass loss rate of $\dot{M}_{\rm burst} = 1 M_\odot$ yr^{-1} for 20 years. The mass is removed from the outer radiative region. This mass loss rate mimics the average mass loss rate during the Great Eruption. We then reduce the mass loss rate to $\dot{M}_p = 2 \times 10^{-4} M_\odot$ yr^{-1}, and follow the star for another 200 years. In Fig. 3 we plot the radius and luminosity of the star as function of time during the eruption.

The mass loss rate during the 20 years eruption proceeds on a time scale much longer than the dynamical time scale, but it is shorter than the thermal time scale. At the beginning of the outburst the stellar radius is $R = 220 R_\odot$. The average thermal time scale of the outer region of mass dm is $\tau_{\rm th} = GMdm/RL$, while the mass loss time scale is $\tau_{\rm ml} = dm/\dot{M}$. Their ratio is

$$\frac{\tau_{\rm th}}{\tau_{\rm ml}} = 7 \left(\frac{M}{140 M_\odot} \right) \left(\frac{\dot{M}}{1 M_\odot \ {\rm yr}^{-1}} \right) \left(\frac{R}{200 R_\odot} \right)^{-1} \left(\frac{L}{3 \times 10^6 L_\odot} \right)^{-1} . \quad (1)$$

The thermal time scale is substantially longer than the mass loss time scale. As a result of this the star losses its thermal equilibrium and rapidly contracts, i.e., on a time scale of few years which is much shorter than the thermal time scale. As our model is not fully built to take into account evolution on time scales shorter than the thermal time scale, e.g., it does not take into account the energy required to remove the mass from the envelope, our results of the rapid mass loss episode are not accurate. The code cannot handle properly the removal of mass during a time shorter than the thermal time scale, and there are large fluctuations in the luminosity and radius. In reality, the star exceeds its Eddington luminosity limit and is expected to be unstable (Shaviv 2001). However, as the mass loss time scale is longer than the dynamical time scale, our results correctly give the general description.

It is evident that as mass loss starts on a timescale shorter than the thermal time scale the inner regions of the star contracts, and release a huge amount of gravitational energy. In our non-dynamical model the released gravitational energy leads to a higher luminosity. In

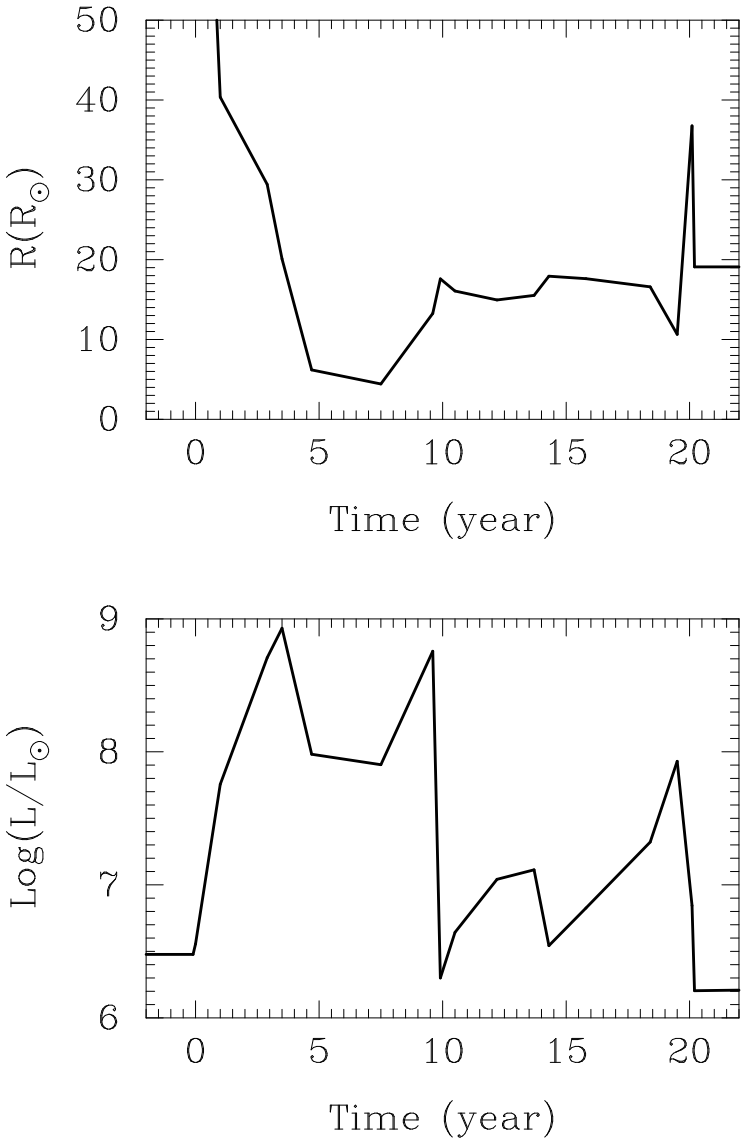

Fig. 3.— The radius and luminosity of the star during the runaway mass loss episode (eruption), starting two years before the high mass loss rate and ending two years after. The pre-outburst radius in our model is $\sim 200 R_\odot$. During the eruption phase, $0 \leq t_e \leq 20$ yr, mass was removed from the outer radiative zone at a rate of $\dot{M}_{\rm burst} = 1 M_\odot$ yr^{-1}. Because the mass loss time scale is shorter than the thermal time scale, the numerical code is unstable, and there are large fluctuations. However, the general shrinkage of the star and the release of a huge amount of energy is evident.

reality, the increased luminosity will result in a higher mass loss rate, even if with a smaller terminal speed than in the regular wind, because the luminosity exceeds the Eddington limit luminosity by more than an order of magnitude. In particular, the opacity of the expelled mass is huge, and the extra luminosity would be absorbed in the wind, and accelerates it. Our model does not have the wind component. Therefore, the luminosity given above is not the observed luminosity, but rather the energy available to accelerate the expelled mass.

The total kinetic energy of the gas in the Homunculus is $\sim 5 \times 10^{49}(M_H/20M_\odot)$ erg where M_H is the mass in the Homunculus (Smith 2006; Soker 2007). The total gravitational energy liberated by the contracting star is $\sim 5 \times 10^{50}$ erg, which is much larger. However, as mentioned, our numerical code does not have in it the energy that is required to remove the mass. After losing only $4M_\odot$ the stellar radius has shrunk to $\sim 15R_\odot$. Losing another $16M_\odot$ from an average radius of $15R_\odot$ requires an energy of $\sim 5 \times 10^{50}$ erg. Namely, most of the energy will go to unbind the expelled gas, and accelerate it. As mentioned earlier, in the binary model (Soker 2001, 2007) the accreting companion can supply most of the energy of the Homunculus, and energy considerations is not of a worry.

Our model is not fully consistent in another manner. The numerical code does not include the triggering process of the high mass loss rate during the eruption. For example, the triggering can come from a tidal interaction with the companion which deposited energy to the envelope. Tidal enhancement of mass loss rate during the Great Eruption was mentioned by Soker (2001), and during present periastron passages by Smith et al. (2003a). Indeed, at the onset of the eruption the stellar radius was $\sim 1AU$, while the periastron distance in η Car is ~ 1.5 AU, implying that a strong tidal interaction took place before and during the onset of the eruption. The primary star could have gone through a weak instability (pulsation) that increased its radius a little. If this continued while the secondary star was at periastron passage, then the secondary could have remove some amount of mass, and trigger the outburst. Another possible triggering process is discussed in the next section.

Although the photospheric radius decreases by more than an order of magnitude during the eruption, mass shells do not contract much. The main contraction of the photosphere is due to removal of the outer high entropy layers. On average, during the 20 years eruption the mass shells at the photosphere (each time a new mass shell) have their radii smaller by a factor of $\zeta_r \leq 2$ than their radii at the beginning of the eruption. This implies that the ratio of rotation velocity to break-up velocity of the mass shells increases by an average factor of only $\zeta_r^{1/2} \simeq 1.5$. In any case, even after contraction the mass shells at the photosphere have their radii larger than their main sequence value. This suggests that a single star cannot posses fast rotation. This discussion further supports the claim that single star models cannot explain the bipolar structure of the Homunculus, and an interaction with a companion is

required (Soker 2004, 2007).

After we terminate the high mass removal rate, i.e., the end of the eruption phase, and set the mass loss rate to $\dot{M}_p = 2 \times 10^{-4} M_\odot$ yr^{-1}, the star relaxes on a very short time, and starts a slow recovery. While during the removal of mass at a high rate the stellar layers contract on average and release gravitational energy, on the recovery phase the star re-expands. This requires energy, and the luminosity is lower than its pre-eruption value. It starts with $L = 1.6 \times 10^6 L_\odot$ immediately after the eruption ends, and increases slowly to $L = 2 \times 10^6 L_\odot$ at 200 years after the eruption. This slow recovery might be related to the secular brightness of η Car. In our model the effective temperature 200 years after the eruption is very high, $T_e \simeq 5 \times 10^4$ K. However, our treatment of the eruption is not accurate, and it is possible that the recovery phase is more rapid than what we find. In any case, the dense wind of the primary in η Car blocks the UV radiation from its photosphere (Hillier et al. 2001, 2006).

4. MAGNETIC ACTIVITY

In §3 we found that an initial rapid mass loss will lead to a runaway process. The initial rapid mass loss might be triggered by a tidal interaction with a companion, or from internal changes in the star. The proximity of the star to its Eddington luminosity limit most probably is also a key property of the star. Here we examine a possible triggering by magnetic fields (Soker 2007).

In the evolved star just prior to eruption, the inner $\sim 80 M_\odot$ region is convective (the convective core), while most of the envelope is radiative. It is quite possible that a dynamo will be operating in the boundary of the convective core and the radiative region above it (e.g., Charbonneau & MacGregor 2001; MacGregor & Cassinelli 2003). This boundary is located where the entropy starts to rise, at $(M, r) = (81 M_\odot, 6 R_\odot)$ in the model presented in the lower panel of Fig. 1 and in Fig. 2. As can be seen, above this radius the entropy rises sharply, until it flatten again in the outer $\sim 20 M_\odot$. The mass of $\sim 20 M_\odot$ above the steep entropy region, is about equal to the mass expelled in the Great Eruption of η Car. In our model this is not a coincidence. In the sun, magnetic flux tubes that are formed in the lower boundary of the convective region buoy outward to the surface. However, in the case studied here the magnetic flux tubes need to buoy through the radiative region, where entropy increases outward. We now examine this situation.

We note that a more thorough study is conducted by MacGregor & Cassinelli (2003) who considered also stellar rotation and heat transfer. The aim of our simpler treatment is

to emphasize the important role that the steep entropy rise in the radiative zone might play in forming a strong magnetic field region.

Consider a magnetic flux tube, or a magnetic flux loop, formed at the bottom of the radiative zone $r = r_0$, with a magnetic field of intensity B_{t0} and density ρ_{t0}, and with an initial temperature equals to the ambient (envelope) temperature $T_{t0} = T_e(r_0) \equiv T_{e0}$ at this radius. The ambient density is ρ_e, and the magnetic field in the ambient medium is assumed to be much weaker than that in the tube (or loop), such that the ambient pressure is $P_e(r) = \rho_e k T_e/\mu m_H$, where μm_H is the mean mass per particle. Let the cross-section of the tube be $A(r)$, with $A_0 \equiv A(r_0)$, and let its length be L. The flux tube and our stellar model just before the eruption are drawn schematically in Fig. 4.

For the evolution of the magnetic field inside the tube we take

$$B_t = B_{t0}\frac{A_0}{A} = B_{t0}\left(\frac{\rho_t}{\rho_{t0}}\right)^{\delta}, \tag{2}$$

where the first equality results from magnetic flux conservation, while the value of δ depends on the relative variation of A and L. If the length of the tube does not change much as it rises, as might be the case if the magnetic field is strong, then $\delta = 1$. If, on the other hand, the field is random or the relative expansion of all dimensions is the same, as expected when the field is weak and it is dragged by the rising tube, then $\delta = 2/3$. We will take here $\delta = 2/3$ as appropriate for a weak initial magnetic field.

We also define the initial ratio of thermal to magnetic pressure inside the tube

$$\beta_0 \equiv \left(\frac{P_{\rm thermal}}{P_B}\right)_{t0} = \frac{\rho_{t0} k T_{t0}}{\mu m_H}\left(\frac{B_{t0}^2}{8\pi}\right)^{-1}. \tag{3}$$

The pressure inside the tube includes magnetic and thermal contributions, and can be written as

$$P_t = P_{\rm thermal} + P_B = \frac{\rho_t k T_t}{\mu m_H} + \frac{B_t^2}{8\pi}. \tag{4}$$

We assume adiabatic evolution of the tube such that the temperature inside the tube evolves as $T_t \propto \rho_t^{\gamma_{\rm ad}-1}$, and use equation (2) to write for the pressure inside the tube

$$P_t = \frac{\rho_{t0} k T_{t0}}{\mu m_H}\left(\frac{\rho_t}{\rho_{t0}}\right)^{\gamma_{\rm ad}} + \frac{B_{t0}^2}{8\pi}\left(\frac{\rho_t}{\rho_{t0}}\right)^{2\delta}. \tag{5}$$

The adiabatic index is not constant in the star. However, as evident from Fig. 2, it is quite constant with $\gamma_{\rm ad} \simeq 4/3$ in the radiative zone above the convective core (because radiation pressure is very important there). In that zone, $6 \lesssim r \lesssim 22 R_\odot$ ($80 \lesssim M \lesssim 120 M_\odot$), the entropy steeply rises by a factor of $S_e(22R_\odot)/S_{e0} = 2.3$ (Fig. 2).

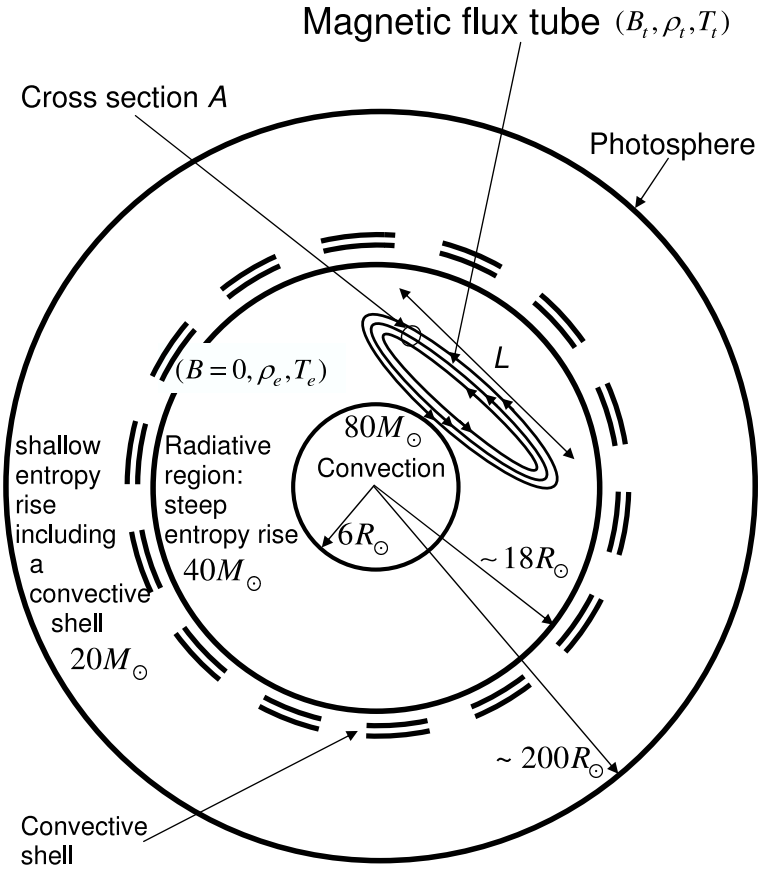

Fig. 4.— Schematic drawing of our stellar model just before the eruption, with a flux loop embedded in the radiative envelope. There is a core convective region in the sphere $r < r_0 = 6R_\odot$, and a second convective shell in the range $22 \lesssim r \lesssim 28R_\odot$ ($127 \lesssim M \lesssim 132M_\odot$).

Using the definition of β_0 we can cast equation (5) into

$$P_t = \frac{P_{e0}}{1+\beta_0^{-1}} \left[\left(\frac{\rho_t}{\rho_{t0}} \right)^{\gamma_{\rm ad}} + \frac{1}{\beta_0} \left(\frac{\rho_t}{\rho_{t0}} \right)^{2\delta} \right], \tag{6}$$

where $P_{e0} = P_{t0} = (1+\beta^{-1})\rho_{t0} k T_{t0}/\mu m_H$, as the tube and ambient pressures at the origin r_0 are equal. Since we assume that the temperature of the tube is equal to the ambient temperature at its origin, we find the expression that connects the density of the tube to the ambient pressure at the origin $\rho_{e0} = (1+\beta^{-1})\rho_{t0}$. As the tube rises, its pressure equals to the ambient pressure $P_t = P_e(r)$. Using these expressions for ρ_{t0} and P_t, in equation (6) gives

$$\frac{P_e(r)}{P_{e0}} = \frac{1}{1+\beta_0^{-1}} \left[\left(\frac{\rho_t}{\rho_{e0}} \right)^{\gamma_{\rm ad}} (1+\beta_0^{-1})^{\gamma_{\rm ad}} + \frac{1}{\beta_0} \left(\frac{\rho_t}{\rho_{e0}} \right)^{2\delta} (1+\beta_0^{-1})^{2\delta} \right]. \tag{7}$$

We now examine the possibility that the flux tube reaches a new equilibrium position, namely, a radius where its density is equal to the ambient (envelope) density $\rho_t = \rho_e(r)$. This will be possible only if the entropy of the envelope increases fast enough with radius. Substituting this equality in equation (7), and dividing by $[\rho_e(r)/\rho_{e0}]^{\gamma_{\rm ad}}$, we find

$$\frac{P_e(r)/[\rho_e(r)]^{\gamma_{\rm ad}}}{P_{e0}/\rho_{e0}^{\gamma_{\rm ad}}} = \left(1+\beta_0^{-1}\right)^{\gamma_{\rm ad}-1} + \left(1+\beta_0^{-1}\right)^{2\delta-1} \frac{1}{\beta_0} \left[\frac{\rho_e(r)}{\rho_{e0}} \right]^{2\delta-\gamma_{\rm ad}}. \tag{8}$$

We take for the envelope entropy $S_e(r) \simeq S_\gamma(r) \equiv P_e/\rho_e^{\gamma_{\rm ad}}$, with $\gamma_{\rm ad} \simeq 4/3$, and for the behavior of the magnetic field $2\delta \simeq 4/3$, and derive from equation (8)

$$\frac{S_e(r)}{S_{e0}} \simeq \left(1+\beta_0^{-1}\right)^{1.33} \tag{9}$$

Rising magnetic flux tubes will stop rising when the equality in equation (9) holds. This situation is not completely stable. MacGregor & Cassinelli (2003) have showed that when heat transfer (by radiative diffusion) and rotation are considered, the flux loops emitted in the equatorial plane can attain a stationary equilibrium stable with respect to small displacements in radius, but are unstable when perturbed in other directions. However, the flux loops move outward on a long time scale (see below). In any case, magnetic field energy can attain a large value in the radiative region with the steep entropy rise. The rise in entropy in the region $6 \lesssim r \lesssim 22 R_\odot$ ($80 \lesssim M \lesssim 120 M_\odot$) is by a factor of $S_e(22R_\odot)/S_{e0} = 2.3$ (Fig. 2). From equation (9) we find then, that the magnetic flux tube will come to rest in this radiative zone if $\beta_0 \gtrsim 1$. Namely, the initial magnetic pressure must be smaller than the thermal pressure in the tube.

The rapid (on several dynamical time scales, or about a year) release of the magnetic energy stored in the radiative region between the two convective regions might trigger a high mass loss rate for a short time, that will then sustain itself and develop to the runaway loss of $> 10 M_{\odot}$ from the envelope, as discussed in the previous section.

If stellar rotation and heat transfer are considered the flux tubes do not reach an equilibrium (MacGregor & Cassinelli 2003). However, the rise of flux loops is determined by heating via radiative diffusion. This heating proceeds on a long time scale, $> 10^4$ yr (MacGregor & Cassinelli 2003), which is longer than the expected time between major LBV eruptions (Smith & Owocki 2006). Even meridional circulation (MacGregor & Cassinelli 2003) will transport the flux loops on a long time scale, much longer than buoyant time scale in a convective region. In our scenario it is assumed that LBV stars posses magnetic activity cycles, and the activity builds itself to a maximum on a time scale shorter than the meridional circulation and heat transfer time scales. The magnetic energy that is stored is required to remove a large amount of mass in a short time to set the runaway mass loss episode.

In addition to the amplification of magnetic fields in the boundary of the inner convective region and the radiative region above it, the outer convective region can also amplify the magnetic field. All these possible dynamo activities are beyond the scope of the present paper. Our only goal is to point to the possibility that LBV large eruptions are triggered by magnetic activity.

5. SUMMARY

Our main goal was to examine the triggering and runaway mass loss process of major eruptions of luminous blue variables (LBVs) stars, e.g., the 1837-1856 Great Eruption of η Car.

We followed the evolution of a massive star. We started with a solar composition and with $[M(M_{\odot}), L(10^6 L_{\odot}), T_e(10^4 K)] = (190, 3, 5.7)$, for the mass, luminosity and effective temperature, respectively. We then evolved the star to almost complete depletion of hydrogen in its core (§2), where the star had $[M(M_{\odot}), L(10^6 L_{\odot}), T_e(10^4 K)] = (139, 3, 1.6)$; our treatment of the atmosphere is not accurate, and for that the effective temperature can be in the range $\sim 15,000 - 20,000$ K. The star has a convective core, then a radiative zone, followed by another convective shell (Figs. 1 and 2). The outer most zone is a very extended radiative one, with very small amount of mass. The most important property of the model is the development of a steep entropy rise above the convective core. The mass of $\sim 20 M_{\odot}$ above the steep entropy region (see lower panel of Fig. 1 and Fig. 4) is about equal to the

mass expelled in the Great Eruption of η Car. In our model this is not a coincidence.

In §3 we studied the response of the star to the eruption phase. We removed $20M_{\odot}$ at a rate of $1M_{\odot}$ yr^{-1}. Numerically, the mass was removed from the outer radiative zone. This mass loss time scale is shorter than the thermal time scale of the star (eq. 1), and before removing even $1M_{\odot}$, the envelope losses its thermal equilibrium. The envelope contracts, and its luminosity increases (Fig. 3). The increase in luminosity that result from the release of gravitational energy is huge. Very likely, this will sustain the high mass loss rate, and develop into a runaway mass loss eruption. Our code is not consistent in that we do not follow the energy required to remove the mass; we simply remove mass from the envelope. Still, we can safely conclude that if a triggering mechanism can remove mass, even a small amount of $\lesssim 0.5M_{\odot}$, within a time much shorter than the thermal time scale of that mass, a runway mass loss process will develop.

It should be noted that although the photosphere shrinks a lot, the motion of mass shells inward is not by a large factor. This implies that the star will not spin-up much during the eruption phase. The formation of a bipolar nebulae seems to require a binary companion.

In §3 we also followed the star for another 200 years after the end of the eruption, with a mass loss rate of $\dot{M} = 2 \times 10^{-4}$ to mimic the behavior of η Car after the Great Eruption. As our treatment of the eruption phase is not fully consistent, we also do not have the correct values for the post-eruption phase. For example, taking into account the energy required to remove the mass from the star would reduce the energy radiated by the star, and would make the envelope shrinkage smaller. The recovery phase after the eruption will be shorter. Still, we managed to show that the star tries to recover from the eruption.

The triggering of the rapid mass loss rate can come from a companion or from internal structural changes. In the case of η Car, a strong interaction with the companion took place, and this could have triggered the eruption. In §4 we examine the possibility that a magnetic activity cycle is the trigger. We showed that a strong magnetic field region can be built in the radiative zone above the convective core, as schematically drawn in Fig. 4. When this energy is released as the magnetic cycle reaches its peak, it can trigger a fast removal of mass, and by that trigger the eruption.

The prediction is that LBV stars that are experiencing major eruptions, should be found to have a close companion, and/or have signatures of strong magnetic activity during or after the eruption.

We thank Nathan Smith for useful comments. This research was supported by grants from the Israel Science Foundation, and from Asher Space Research Institute at the Technion.

REFERENCES

Charbonneau, P., & MacGregor, K. B. 2001, ApJ, 559, 1094

Davidson, K., & Humphreys, R. M. 1997, ARA&A, 35, 1

Heisler, J., & Alcock, C. 1986, ApJ, 306, 166

Hillier, D. J., Davidson, K., Ishibashi, K., & Gull, T. 2001, ApJ, 553, 837

Hillier, D. J., Gull, T., Nielsen, K., Sonneborn, G., Iping, R., Smith, N., Corcoran, M., Damineli, A., Hamann, F. W., Martin, J. C., & Weis, K. 2006, ApJ, 642, 1098

Humphreys, R. M., & Davidson, K. 1994, PASP, 106, 1025

Humphreys, R. M., Davidson, K., & Smith, N. 1999, PASP, 111, 1124

MacGregor, K. B., & Cassinelli, J. P. 2003, ApJ, 586, 480

Maeder, A. 1992, in Instabilities in Evolved Super- and Hyper-giants stars, ed. C de Jager and H. Nieuwenhuijzen (Amsterdam, North-Holland), 138.

Meynet, G. & Maeder, A. 2003, A&A, 404, 975

Meynet, G. & Maeder, A. 2005, A&A, 429, 581

Owocki, S., Gayley, K., & Shaviv, N. 2004, ApJ 616, 525

Owocki, S., & van Marle, A. J. 2009, in Massive Stars as Cosmic Engines, IAU Sym. 250, eds. F. Bresolin, P. Crowther & J. Puls, (arXiv:0801.2519)

Shaviv, N. 1998, ApJ 494, L193

Shaviv, N. 2000, ApJ 529, L137

Shaviv, N. 2001, ApJ 549, 1093

Smith, N. 2006, ApJ, 644, 1151

Smith, N. & Conti, P. S. 2008, ApJ, 679, 1467

Smith, N. Davidson, K., Gull, T. R., Ishibashi, K., Hillier, D. J. 2003a, ApJ, 586, 432

Smith, N., & Ferland, G. J. 2007, ApJ, 655, 911

Smith, N., Gehrz, R., D., Hinz, P. M., Hoffmann, W. F., Hora, J. L., Mamajek, E. E., & Meyer, M. R. 2003b, AJ, 125, 1458

Smith, N., & Morse, J. A. 2004, ApJ, 605, 854

Smith, N., & Owocki, S. P. 2006, ApJ, 645, L45

Soker, N. 2001, MNRAS, 325, 584

Soker, N. 2004, ApJ, 612, 1060

Soker, N. 2007, ApJ, 661, 490

Soker, N., & Harpaz, A. 1999, MNRAS, 310, 1158

van Marle, A. J., Owocki, S. P. & Shaviv, N. J. 2008, MNRAS, 389, 1353

van Marle, A. J., Owocki, S. P. & Shaviv, N. J. 2009, MNRAS, in press (arXiv:0812.0242)

Webbink, R. F. 1976, ApJS, 32, 583

This preprint was prepared with the AAS LaTeX macros v5.2.